

# Broadband Gap-coupled Shorted 60° Sectoral Microstrip Antenna

Amit A. Deshmukh  
Professor and Head, EXTC Dept.,  
DJ Sanghvi College of Engineering  
Vile Parle (W) Mumbai, India

Shafin B. Nagarbowdi, N. V. Phatak,  
A. A. Desai, S. A. Shaikh, K. A. Lele, S.  
Agrawal  
PG student, EXTC Dept.,  
D. J. Sanghvi College of Engineering  
Vile Parle (W) Mumbai, India

## ABSTRACT

The compact variation of equilateral triangular microstrip antenna, a shorted 60° Sectoral microstrip antenna is discussed. The proximity fed shorted 60° Sectoral microstrip antenna is proposed which gives simulated and measured BW of more than 700 MHz (>60%). To increase the bandwidth and gain, gap-coupled configuration two Shorted 60° Sectoral patches is proposed. It yields simulated and measured bandwidth of more than 800 MHz (>70%). Due to shorted patch, single and gap-coupled shorted Sectoral configurations shows higher cross polar radiation pattern with gain of more than 3 dBi and more than 4 dBi, respectively over the bandwidth. Although the antenna shows higher cross polar levels, but the proposed designs in 800 to 1400 MHz frequency range can find applications in mobile communication environment wherein higher cross polar content will lead to lower signal loss.

## Keyword

Equilateral triangular microstrip antenna, Compact microstrip antenna, Shorted 60° Sectoral microstrip antenna, Gap-coupled, Proximity feed

## 1. INTRODUCTION

The simplest method to realize broadband microstrip antenna (MSA) is by designing the patch on air substrate of thickness more than  $0.06\lambda_0$ , in conjunction with the proximity feeding technique [1 – 5]. The air has dielectric constant of unity that reduces the quality factor of the cavity below the patch whereas proximity feeding yields input impedance matching while using thicker substrate, which together yields broadband response. The bandwidth (BW) of suspended MSAs is further increased by using multi-resonator gap-coupled configuration in which parasitic patches of different frequencies (dimensions) are gap-coupled to the fed MSA. The compact MSA is realized by placing the shorting post/plate along the zero field line at the fundamental patch mode and further by using half of the shorted patch [1 – 3]. The BW of compact shorted MSA is increased by using their gap-coupled configurations [6]. The compact variations of equilateral triangular MSA (ETMSA) are realized by placing the shorting post along the zero field line at its fundamental  $TM_{10}$  mode [1 – 3]. This result in compact shorted 60° Sectoral and complementary of shorted 60° Sectoral MSAs. The shorted Sectoral patch yields nearly 60% whereas complementary configuration yields nearly 40% reduction in patch size as compared to ETMSA.

In this paper, broadband gap-coupled variation of proximity fed shorted 60° Sectoral MSA is proposed. First the proximity fed shorted 60° Sectoral MSA is studied. It yields simulated and measured BW of more than 700 MHz (>60%). The single shorted patch yields gain of more than 3 dBi over most of the BW. Due to shorted patch, radiation pattern shows higher cross-polar levels. Further a gap-coupled configuration of two shorted 60° Sectoral MSAs is proposed. It gives simulated and measured BW of more than 800 MHz (>70%) with gain of more than 4 dBi over most of the BW. The gap-coupled compact configuration is proposed in 1000 MHz frequency band. This frequency band is chosen since % antenna BW is smaller at individual modes in this range. To realize broader BW and maximum radiation efficiency, compact MSAs were optimized on air substrate of thickness 3.0 cm ( $\geq 0.1\lambda_0$ ). The proximity feeding technique is used to feed the MSAs, since it is a simpler method to implement on thicker substrates. The compact shorted MSAs were first optimized using IE3D software [7]. For experimental verification the MSA were fabricated using copper plate having finite thickness and were supported in air using foam spacer support place towards the antenna corners. The antenna is fed using N-type connector of 0.32 cm inner wire diameter. The measurement was carried out using R & S vector network analyzer on finite square ground plane of side length 30 cm. The radiation pattern were measured in minimum reflection surrounding with required minimum far field distance between reference antenna and the antenna under test [8]. The gain was measured using two antenna method [8].

## 2. PROXIMITY FED SHORTED 60° SECTORAL MSAs

The proximity fed ETMSA is shown in Fig. 1(a, b). The units of the dimension shown in all the figures and their captions are in cm. Also the frequencies mentioned throughout the text and in the figures are in MHz. For  $h = 3.0$ , using the resonance frequency equation of ETMSA as given in equation (1), patch side length (S) is calculated such that its  $TM_{10}$  mode frequency is around 1000 MHz.

$$f_{TM_{10}} = \frac{2c\sqrt{m^2 + nn + n^2}}{3S_e\sqrt{\epsilon_{re}}} \quad (1)$$

Where,  $c$  = velocity of light =  $3 \times 10^8$  (m/s),

$S_e$  = effective patch side length,  
 m and n = mode indices

While calculating the frequency, the effective patch side length ( $S_e$ ) needs to be considered. The effective length accounts for extension in length due to fringing fields present towards the open circuit edges of the patch side length. The closed form equation for fringing field extension length is not directly available for thicker substrate hence patch side length cannot be accurately calculated for different frequencies and for thicker substrate. The artificial neural network model to calculate the patch side length and extension length in terms of substrate thickness in ETMSA, for substrate thickness varying from  $0.04$  to  $0.1\lambda_0$  and for frequency changing from  $700$  to  $6000$  MHz is reported [9]. Using the same patch side length that gives  $f_{TM_{10}}$  around  $950$  MHz is calculated and it is found to be  $13.8$  cm. In ETMSA, field variations are symmetrical with respect to patch centroid point. At  $TM_{10}$  mode field/surface current shows one half wavelength variations along patch side length and along its height, with zero field at the centroid point. The next mode in ETMSA is  $TM_{11}$ . Depending upon the feed position, at  $TM_{11}$  mode, field shows one half wave length variations from the centroid point and towards the patch vertex. The next higher order mode is  $TM_{20}$ , at which field shows two half wavelength variations along the side length and along height of the patch. At  $TM_{10}$  mode, compact shorted  $60^\circ$  Sectoral MSA is derived by placing the shorting plate along the zero field line of  $TM_{10}$  mode and by using half of the shorted patch, as shown in the Fig. 1(c). The dominant mode in shorted  $60^\circ$  Sectoral MSA is shorted  $TM_{10}$  at which surface current shows quarter wavelength variation along shorted Sectoral length as shown in Fig. 1(d). This mode is also referred to as  $TM_{1/4,0}$  mode. Here the first index corresponds to odd integer multiples of quarter wavelength variation along shorted length (mixed boundary condition) and the second index refers to integer multiples of half wavelength variations along the orthogonal shorted patch dimension (identical boundary condition). The shorted  $TM_{20}$  mode is also present in shorted  $60^\circ$  Sectoral MSA as it also shows zero fields near the centroid point. At shorted  $TM_{20}$  mode currents shows three quarter wavelength variation along shorted sector length as shown in Fig. 1(e). The radius of shorted  $60^\circ$  Sectoral MSA is  $8.0$  cm. To optimize the shorted configuration for broader BW, parametric study for variation in thickness of coupling strip and its position below the shorted patch is carried out. The input impedance locus for  $h = 3.0$ ,  $h_1 = 2.8$ ,  $l_s = 2.8$  and  $x_f = 4.0$  is shown in Fig. 1(f). The loop position is not optimized for broader BW.

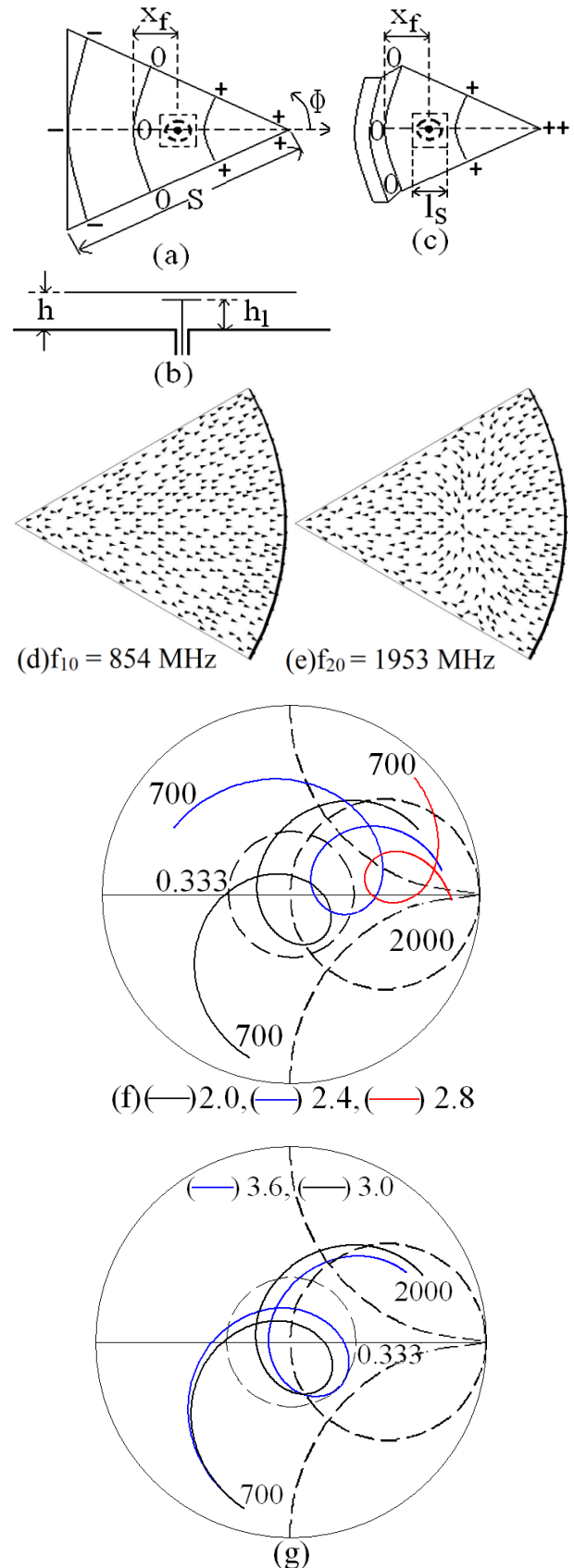
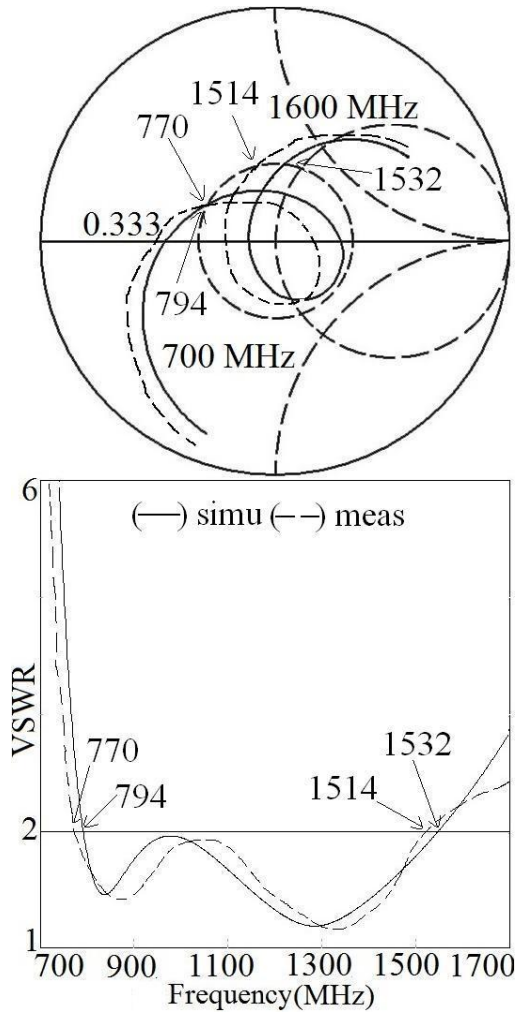


Fig. 1 (a) Top and (b) side views of proximity fed ETMSA, (c) shorted  $60^\circ$  Sectoral MSA, its (d, e) surface current distribution at two modes and its input impedance plots for variation in (f)  $h_1$  and (g)  $x_f$

To optimize the loop position, substrate thickness for strip ( $h_1$ ) is reduced and impedance plots for the same are shown in Fig. 1(f). The reduction in  $h_1$  increases the capacitive impedance between strip and patch which rotates the loop position in anti-clockwise in the smith chart. The loop lies inside VSWR = 2 circle for  $h_1 = 2.0$  cm. However loop size is smaller. To increase the same, strip is placed below the higher impedance region below the shorted patch. The impedance plots for variation in strip position ( $x_f$ ) are shown in Fig. 1(g). The loop size increases due to increase in  $x_f$ . This gives simulated BW of 738 MHz (63.5%) whereas the measured BW is 744 MHz (65.1%) as shown in Fig. 2.



**Fig. 2 Input impedance and VSWR plots for proximity fed shorted 60° Sectoral MSA**

Due to shorted patch, radiation pattern shows higher cross polar levels with gain of around 3 dBi over most of the BW. To further increase the gain and BW gap-coupled configuration of two shorted 60° Sectoral MSAs is proposed as shown in Fig. 3(a, b). The radius of parasitic shorted 60° Sectoral MSA is taken to be smaller than the fed patch radius. The resonance curve plots for decreasing parasitic patch radius are shown in Fig. 3(c). With decrease in radius, frequency of parasitic shorted 60° Sectoral MSA increases. The optimum spacing between two frequencies to realize broader BW is obtained for radius of 6.0 cm. The input

impedance and VSWR plots for the same are shown in Fig. 4(a). Due to two resonant modes, two loops are present inside VSWR = 2 circle.

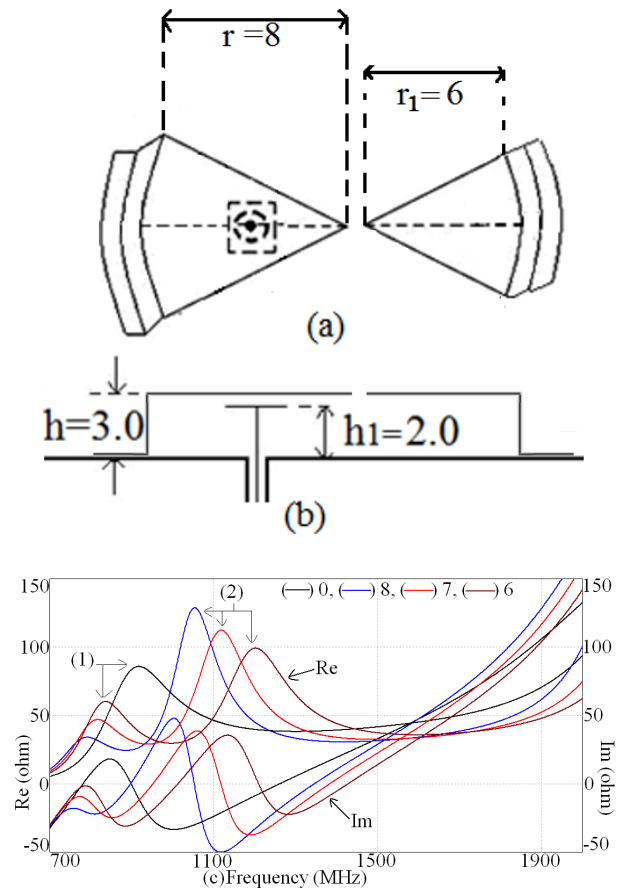
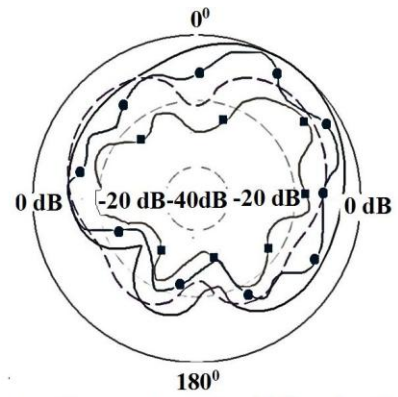
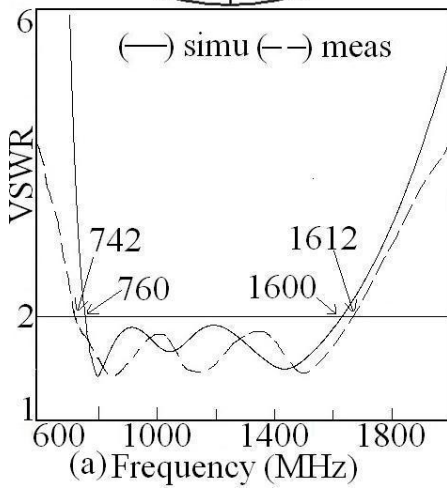
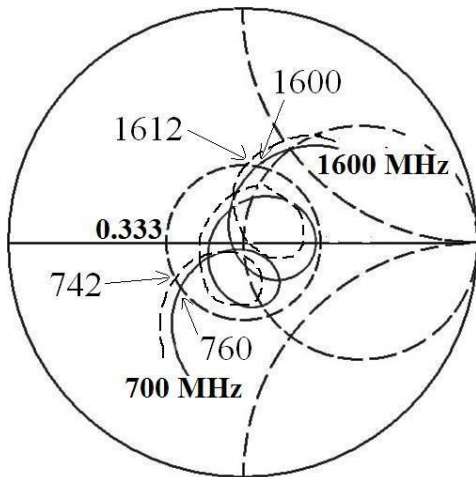
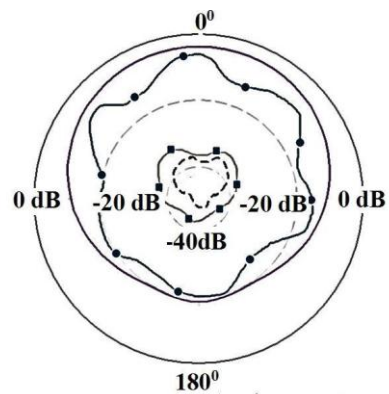


**Fig. 3 (a) Top and (b) side views of proximity fed gap-coupled shorted 60° Sectoral MSAs and its (c) resonance curve plots for varying radius 'r<sub>1</sub>'**

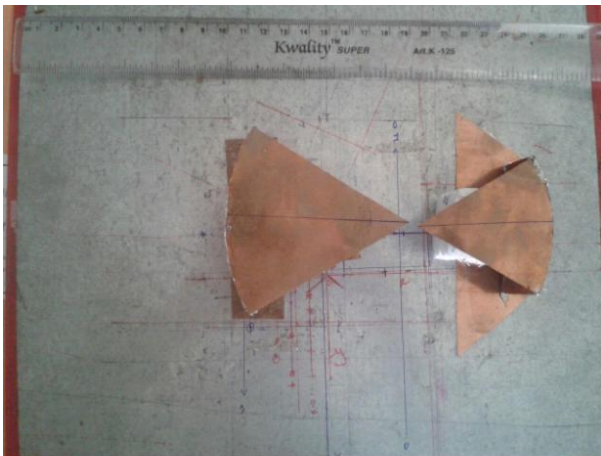
The simulated and measured BW's are, 840 MHz (71.2%) and 870 MHz (73.9%). The fabricated prototype of the gap-coupled configuration is shown in Fig. 4(b). The simulated and measured radiation pattern at center frequency of the BW and gain variation over the BW is shown in Fig. 5(a – c). The pattern is in the broadside direction with higher cross polar levels in E-plane. This is because in E-plane, field distribution is more un-symmetrical as compared to that in the H-plane. The antenna gain is more than 4 dBi over most of the BW. The area of the proposed gap-coupled configuration is 53 cm<sup>2</sup>. The proximity fed ETMSA yields simulated and measured BW of more than 350 MHz (>30%) at its TM<sub>10</sub> mode frequency to be around 950 MHz. The area of ETMSA is 83 cm<sup>2</sup>. The U-slot or rectangular slot cut variations of this proximity fed ETMSA yields simulated and measured BW of more than 500 MHz (>45%). Thus the proposed gap-coupled configuration of shorted 60° Sectoral MSA yields much higher BW with 36% reduction in patch area. Although they shows higher cross polar radiation pattern, but it may be useful in mobile communication environment as higher cross polar content will lead to lesser signal loss.



— E-Copolar Simulated —●— E-Copolar Measured  
 - - - E-Crosspolar Simulated - - - E-cross polar Measured  
 (a)  $f = 1179$  MHz



— H-Copolar Simulated —●— H-Copolar Measured  
 - - - H-Crosspolar Simulated - - - H-cross polar Measured  
 (b)  $f = 1179$  MHz



(b)

Fig. 4 (a) Input impedance and VSWR plots and (b) fabricated prototype of proximity fed gap-coupled shorted  $60^\circ$  Sectoral MSAs

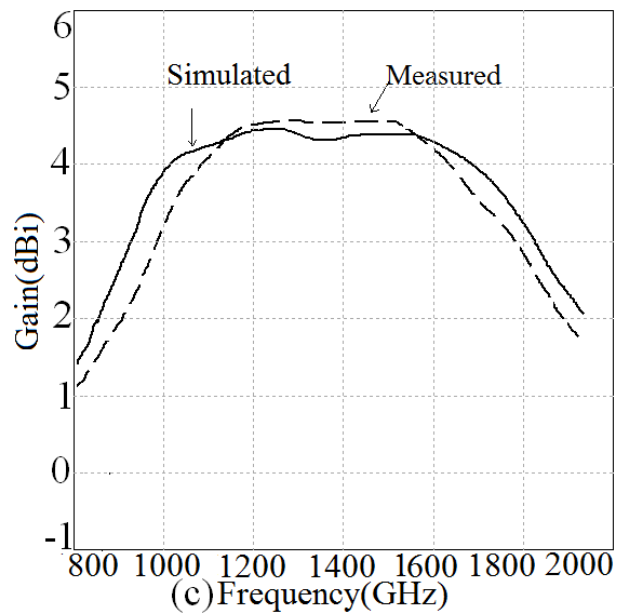


Fig. 5 (a, b) Radiation pattern at center frequency and (b) gain variation over BW for proximity fed gap-coupled shorted  $60^\circ$  Sectoral MSAs

### 3. CONCLUSIONS

The broadband gap-coupled proximity fed shorted 600 Sectoral MSA is proposed. The gap-coupled configuration yields more than 70% BW as compared to more than 35% and more than 45% BW realized in ETMSA and their slot cut variation with 36% reduction in patch area. Due to shorted patch the radiation pattern shows higher cross polar levels but they will be useful in applications wherein multipath propagation effects affects polarization purity of the received signal.

### 4. REFERENCES

- [1] Garg, R., Bhartia, P., Bahl, I., Ittipiboon, A., 2001. *Microstrip Antenna Design Handbook*, Artech House, USA.
- [2] Kumar, G., Ray, K. P., 2003. *Broadband Microstrip Antennas*, 1st edn., Artech House, USA.
- [3] B. Bhartia and I. J. Bahl, *Microstrip Antennas*, USA, 1980.
- [4] Wong, K. L., 2002. *Compact and Broadband Microstrip Antennas*, 1st edn., John Wiley & sons, Inc., New York, USA.
- [5] Cock, R. T., and Christodoulou, C. G., Design of a two layer capacitively coupled, microstrip patch antenna element for broadband applications, *IEEE Antennas Propag. Soc. Int. Symp. Dig.*, vol. 2, 1987, pp. 936-939.
- [6] Deshmukh, Amit A., and Kumar, G., Compact Broadband gap-coupled Shorted L-shaped Microstrip Antennas, *Microwave and Optical Technology Letters*, vol. 47, no. 6, 20<sup>th</sup> Dec. 2005, pp. 599 – 605.
- [7] IE3D 12.1, Zeland Software, Freemont, USA, 2004.
- [8] Balanis, C. A., *Antenn Theory: analysis and design*, 2<sup>nd</sup> edition, John Wiley & Sons Ltd.
- [9] Deshmukh, Amit A., Venkata, A. P. C., Kulkarni, S. D., and Nagarbowdi, S., Artificial Neural Network Model for Suspended Equilateral Triangular Microstrip Antennas, *Proceedings of ICCICT - 2015*, 15<sup>th</sup> - 17<sup>th</sup> January 2015, Mumbai, India